AUTHOR QUERY FORM

AIP Publishing	Journal: Appl. Phys. Lett. Article Number: 114401APL	Please provide your responses and any corrections by annotating this PDF and uploading it according to the instructions provided in the proof notification email.

Dear Author,

Below are the queries associated with your article; please answer all of these queries before sending the proof back to AIP.
Please indicate the following:
Figures that are to appear as color online only (i.e., Figs. 1, 2, 3) ______________________ (this is a free service).
Figures that are to appear as color online and color in print______________________ (a fee of $325 per figure will apply).

Article checklist: In order to ensure greater accuracy, please check the following and make all necessary corrections before returning your proof.

1. Is the title of your article accurate and spelled correctly?
2. Are the author names in the proper order and spelled correctly?
3. Please check affiliations including spelling, completeness, and correct linking to authors.
4. Did you remember to include acknowledgment of funding, if required, and is it accurate?

Location in article	Query / Remark: click on the Q link to navigate to the appropriate spot in the proof. There, insert your comments as a PDF annotation.
AQ1	Please check the changes made in affiliation 1.
AQ2	We have kept the digits closed-up to the opening paranthesis in Tables I and II, for consistency. Please verify.
AQ3	We have inserted multiplication symbol throughout the first column of Table III. Please verify.
AQ4	Please reword the sentence beginning with "On the other hand,..." so that your meaning will be clear to the reader.
AQ5	We have changed "Hassan 1^er^" as "Hassan 1er" in affiliation and acknowledgments. Please verify.
AQ6	Please verify the change in page number in Refs. 6 and 21.
AQ7	We were unable to locate a digital object identifier (doi) for Ref(s) 15 and 17. Please verify and correct author names and journal details (journal title, volume number, page number, and year) as needed and provide the doi. If a doi is not available, no other information is needed from you. For additional information on doi's, please select this link: http://www.doi.org/
AQ8	We have changed "40KV" as "40 kV." Please check and confirm.

Thank you for your assistance.

APPLIED PHYSICS LETTERS **104**, 000000 (2014)

Phase transitions in heated Sr_2MgTeO_6 double perovskite oxide probed by X-ray diffraction and Raman spectroscopy

Bouchaib Manoun,[1,a)] Y. Tamraoui,[1] P. Lazor,[2] and Wenge Yang[3]

[1]*Equipe Ingénierie et environnement, Laboratoire de Chimie Appliquée et Environnement,*
AQ1 *Universite Hassan 1er, Settat 26000, Morocco*
[2]*Department of Earth Sciences, Uppsala University, SE-752 36 Uppsala, Sweden*
[3]*High Pressure Synergetic Consortium, Geophysical Laboratory, Carnegie Institution of Washington, Argonne, Illinois 60439, USA and High Pressure Science and Technology Advanced Research (HPSTAR), Shanghai 201203, People's Republic of China*

(Received 25 September 2013; accepted 15 December 2013; published online xx xx xxxx)

Double-perovskite oxide Sr_2MgTeO_6 has been synthetized, and its crystal structure was probed by the technique of X-ray diffraction at room temperature. The structure is monoclinic, space group *I*2/*m*. Temperature-induced phase transitions in this compound were investigated by Raman spectroscopy up to 550 °C. Two low-wavenumber modes corresponding to external lattice vibrations merge at temperature of around 100 °C, indicating a phase transition from the monoclinic (*I*2/*m*) to the tetragonal (*I*4/*m*) structure. At 300 °C, changes in the slopes of temperature dependencies of external and O–Te–O bending modes are detected and interpreted as a second phase transition from the tetragonal (*I*4/*m*) to the cubic (*Fm*-3*m*) structure.
[http://dx.doi.org/10.1063/1.4860515]

The perovskite structure has the potential to accommodate huge varieties of ions with multiple ion substitution for a single or several original cations. The double perovskites of the type $A_2MM'O_6$ (where A represents an alkaline earth cation, and M and M" are two heterovalent transition-metal elements) are derived from AMO_3 perovskites, when half of the six coordinated M-site cations are replaced by suitable M" cations. These include manganites, tungsten, or molybdate perovskites, these compounds exhibit diverse properties, such as ferroelectricity, piezoelectricity, non-linear optical properties, and even superconductivity.[1–3] The renewed interest in these compounds arise recently because of the discovery of room temperature colossal magneto-resistance (CMR) property in Sr_2FeMoO_6 compound.[4,5] Owing to their excellent electrical and magnetic applications, great progress relating to different aspects of double perovskites has been made in the last decade. In addition to their technological applications, the fundamental understanding of the structure stability and phase transition under different temperatures is very important for optimizing the next generation of electronics with tailored properties.

Extensive research has been carried out to investigate the properties of $A(B''_{1/3}B''_{2/3})O_3$ perovskites, like $Ba(Mg_{1/3}Ta_{2/3})O_3$ and $Ba(Zn_{1/3}Ta_{2/3})O_3$, as they possess excellent microwave dielectric properties;[6,7] However, less attention has traditionally been paid to microwave dielectric properties of $A(B''_{1/2}B''_{1/2})O_3$ double perovskites. Recently, tellurium-based dielectric ceramics showed excellent microwave properties with very low sintering temperatures (<700 °C);[8–11] however, in most of these materials reported in the literature, Te exists in the 4+ valence state. The existence of A_2MgTeO_6 (A = Sr, Pb, Ba) compounds with Te being oxidized to the 6+ valence state has been reported as a stable perovskite structure with space group *Fm*-3*m*.[12] Later on, Dias *et al.*[13] investigated the vibrational spectroscopic and microwave dielectric properties of A_2MgTeO_6 (A = Sr, Ba, Ca) ceramics. X-ray diffraction (XRD), Raman and infrared spectroscopic investigations of Sr_2MgTeO_6 reported that the Sr-based compound has tetragonal structure with space group *I*4/*m*. These findings were later confirmed with electron diffraction.[14] Very recently, Ubic *et al.* re-examined the crystal structure of Sr_2MgTeO_6 compound using X-ray diffraction, transmission electron microscopy, and scanning electron microscopy methods.[15] Based on the observed symmetries and superlattice reflections in electron diffraction patterns, the structure appears like a pseudotetragonal phase, but the structure which describes it best is monoclinic with space group *I*2/*m:* Rather than undergoing an antiphase-to-in-phase tilt transition along the long axis, a more energy favorable untilted-to-in-phase tilt transition was found, which lowers the symmetry of Sr_2MgTeO_6 to monoclinic, *I*2/*m*. The results are inconsistent with the previous works by Dias *et al.* and Ubic *et al.*, so three different works led to three different symmetries: Cubic, tetragonal, and monoclinic. In this Letter, we investigated the crystal structure of Sr_2MgTeO_6 samples using X-ray diffraction, and then a high temperature study was performed in order to study phase transitions that may occur in this compound. As X-ray diffraction is powerful tool for structural determination and different Raman modes are sensitive to local bonding symmetry, we expect that the combination of these two tools would provide us an ultimate solution for the structural stability and possible phase transition for this system. One hypothesis is that if only one transition will be observed, then the work done by Dias *et al.*[13] and Ubic *et al.*[14] is confirmed (in this case, the transition will be tetragonal to cubic). If two transitions will be observed, then study carried out by Ubic *et al.*[15] will likely prove correct (in this case, the transitions

[a)]Author to whom correspondence should be addressed. Electronic mail: manounb@gmail.com

are monoclinic to tetragonal to cubic). An absence of a phase transition will validate Bayer's work.[12]

The standard method of solid-state chemical reaction was applied to synthesize Sr_2MgTeO_6 compound. Proper stoichiometric molar ratios of the starting compounds were mixed according to the following chemical reaction:

$$2SrCO_3 + MgO + TeO_2 + 1/2\,O_2 \rightarrow Sr_2MgTeO_6 + 2CO_2 \uparrow$$

The starting compounds (supplied by Sigma-Aldrich) were used as received and had the following purities: $SrCO_3$, 99.995%; TeO_2, 99+%; and MgO, 99.995%. The starting materials were mixed and ground in an agate mortar and heated in air in alumina crucibles. The following heat treatment procedure was used: 24 h at 900 °C; 24 h at 1000 °C; and 48 h at 1100 °C. After each heating treatment, the sample was cooled down to room temperature, slowly at 3 °C/min and re-ground (re-mixed) to improve homogeneity. X-ray diffraction measurements were performed after each heat treatment to check the quality of the obtained materials.

The structural refinements were undertaken from the powder data. Diffraction data were collected at room temperature on a D2Phaser (θ-θ) diffractometer. The experimental parameters are: Bragg-Brentano geometry; diffracted-beam graphite monochromator; CuKα radiation (40 kV, 40 mA); Soller slits of 0.02 rad on incident and diffracted beams; divergence slit of 0.5°; antiscatter slit of 1°; and receiving slit of 0.1 mm; with sample spinner. The patterns were scanned through steps of 0.010142 deg (2θ), between 15 and 100 deg (2θ) with a fixed-time counting. The full pattern refinements were carried out by the Rietveld method with the Fullprof program[16] integrated in Winplotr software.[17] The Rietveld refinement of the observed powder XRD data is initiated with scale and background parameters, and, successively, other profile parameters are included. The background is fitted with a fifth order polynomial. The peak shape is fitted with a Pseudo–Voigt profile function. After an appreciable profile matching, the position parameters and isotropic atomic displacement parameters of individual atoms were also refined.

Experiments have been carried out using Raman spectroscopic system designed and built at the Department of Earth Sciences, Uppsala University; the principal layout scheme of the Raman experimental setup is described in Refs. 18 and 19. The key system components include a high-throughput, single stage imaging spectrometer (HoloSpec f/1.8i, Kaiser Optical Systems, Inc.), equipped with a holographic transmission grating and thermoelectrically cooled two-dimensional multichannel CCD detector (Newton, Andor Technology, 1600×400 pixels, thermoelectrically cooled down to -60 °C), a diode-pumped solid-state laser (Cobolt Samba, 532 nm, up to 150 mW), and an optical imaging system (magnification 20×, spatial resolution ~1 μm). Set of holographic filters (SureBlock + NoiseBlock, Ondax) blocked the Rayleigh line. The spectrometer was calibrated by the fluorescence lines of a neon lamp. Non-polarized Raman spectra were collected in back-scattering geometry, in the range of -760 to $+1680\,cm^{-1}$, at a resolution of about $3\,cm^{-1}$. Accuracy and precision of spectral measurements, as estimated from the wavelength calibration procedure and peak fitting results, were $1.5\,cm^{-1}$ and 0.1–$0.3\,cm^{-1}$, respectively. The acquisition time was set to 15 s. Heating was accomplished by using a mica-insulated band heater (DuraBand, Tempco Electric heater Corporation) mounted around the sample ceramic holder and connected to a variable transformer. Temperature changes during the heating/cooling cycles were induced and controlled by adjusting the transformer's voltage (0–240 V) and monitored with an accuracy of ±1 °C by the K-type thermocouple adjacent to the sample. During the spectral acquisitions, temperatures were stabilized to within 1 and 3 °C, for the low and high temperature measurements, respectively.

Indexing of X-ray powder diffraction pattern was performed by means of the computer program Dicvol.[20] The first 15 peak positions, with a maximal absolute error of 0.03° (2θ), were used as input data. The X-ray diffraction patterns were assigned to a monoclinic symmetry with the lattice parameters, that were refined using the complete powder diffraction data sets, a = 5.6102(2) Å, b = 5.5944(2) Å, c = 7.9045(2) Å, and β(°) = 89.998(8).

The X-ray powder patterns were fitted to the calculated ones using the Fullprof program[16] integrated in Winplotr software[17] to minimize the profile discrepancy factor Rp. The refinement of the powder XRD pattern was carried out with monoclinic lattice (I2/*m*) with starting model taken from Fu *et al.*[21] In this model, Sr^{2+}, Mg^{2+}, and Te^{6+} are placed at 4i (x, 0.5, z), 2a (0.5, 0, 0) and 2b (0, 0.5, 0) sites, respectively; the oxygen atoms occupy 4i(x, 0, z) and 8j(x, y, z) positions. Figure 1 illustrates the typical Rietveld refinement patterns

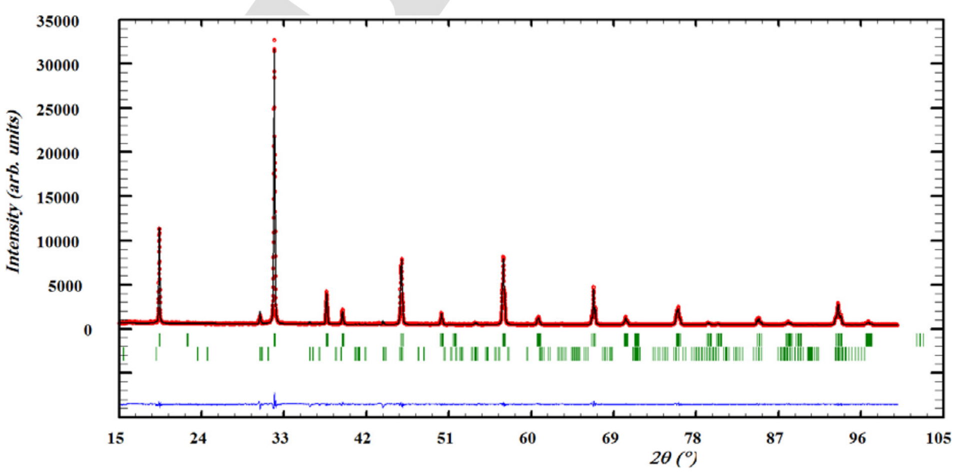

FIG. 1. Final Rietveld plots for monoclinic Sr_2MgTeO_6. The upper symbols illustrate the observed data (circles) and the calculated pattern (solid line). The vertical markers show calculated positions of Bragg reflections. The lower curve is the difference diagram. The non-indexed peaks are unidentified. The refined impurity is $MgTeO_4$.

AQ2

TABLE I. Details of Rietveld refinement parameters for Sr_2MgTeO_6-monoclinic phase.

X-ray wavelength (Å)	$\lambda k\alpha_1 = 1.5406$
2Θ step scan increment (°)	0.010142
2Θ range (°)	15–100
Refinement program	FULLPROF
2Θ zero point offset (°)	−0.0291(10)
Pseudo-Voigt function PV = η L + (1 − η) G	η = 0.5964(77)
Caglioti parameters	U = 0.0286(23)
	V = −0.0074(20)
	W = 0.0074(5)
No. of reflections	152
No. of refined parameter	29
Space group	*I*2/*m*
a (Å)	5.6102(2)
b (Å)	5.5944(2)
c (Å)	7.9045(2)
β (°)	89.9984(83)
V (Å^3)	248.086(9)
Z	2
Atom number	4
RF	4.78
RB	2.76
Rp	3,86
Rwp	5.23
cRp	4.60
cRwp	7.09

TABLE II. Details of Rietveld refinement conditions of the monoclinic Sr_2MgTeO_6.

Atom	X	y	Z	B(Å^2)	Occ
Sr	0.5025(26)	0.5000	0.2505(6)	0.928(6)	2
Mg	1/2	0	0	0.781(21)	1
Te	0	1/2	0	0.670(5)	1
O1	0.5318(55)	0	0.2639(22)	1.004(20)	2
O2	0.2409(26)	0.2576(22)	0.0199(30)	1.004(20)	4

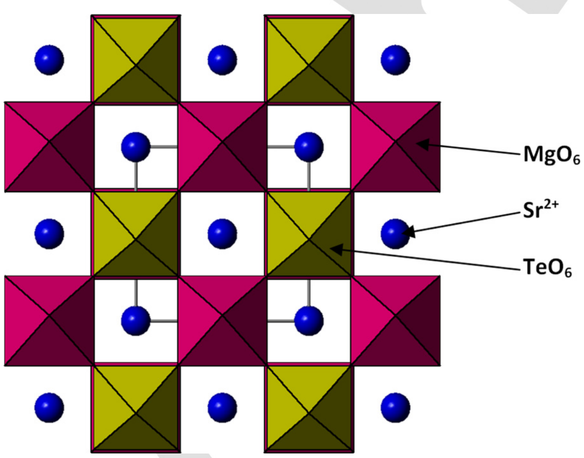

FIG. 2. A (0 0 1) projection of the unit cell indicates the typical polyhedral arrangement.

along with the difference plot at ambient temperature; close inspection of the observed and calculated patterns revealed good agreement between the patterns. Significantly, good residuals of the refinements are obtained (Table I). The refined

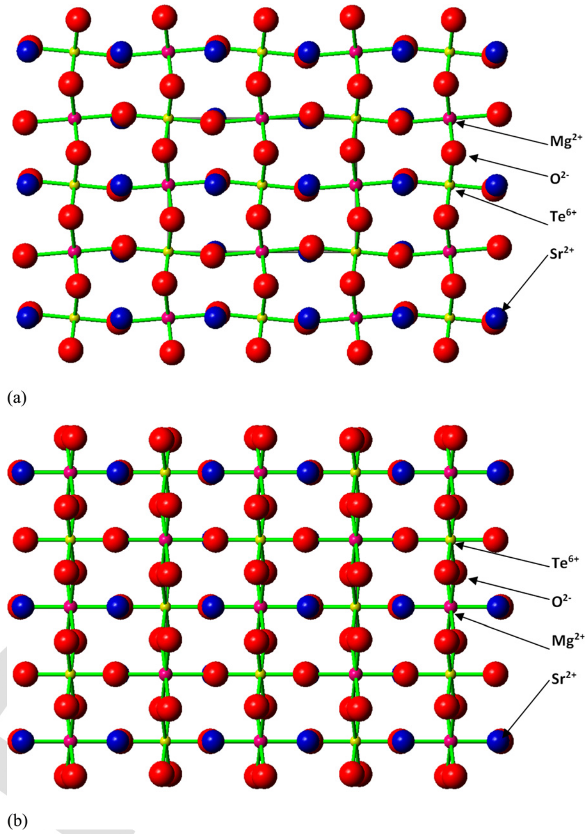

FIG. 3. (0 1 0) (a) and (1 0 0) (b) projections of the unit cell illustrate the typical polyhedral arrangement and the tilt pattern.

position coordinates for the monoclinic Sr_2MgTeO_6, along with other crystallographic data, are given in Table II.

The analysis of refined crystallographic parameters indicates that the Mg^{2+} and Te^{6+} are octahedrally coordinated with the oxygen atoms. The MgO_6 and TeO_6 octahedra are alternatively connected and extended in three dimensions. (0 0 1), (0 1 0), and (1 0 0) projections of the unit cell indicating the typical polyhedral arrangement and the tilt pattern are shown in Figs. 2 and 3. The analysis of inter-atomic distances (Table III) shows that Sr atoms form SrO_{12} polyhedra with the Sr–O bond lengths ranging between 2.606 and 3.007 Å, and the average d value is around 2.802 Å. The

AQ3

TABLE III. Selected inter-atomic distances (Å) and O-Te-O angles for Sr_2MgTeO_6.

2 × Te-O1	1.90423
4 × Te-O2	1.94091
2 × Mg-O1	2.06518
4 × Mg-O2	2.03171
2 × Sr-O1	2.80323
1 × Sr-O1	3.00691
1 × Sr-O1	2.60590
2 × Sr-O2	2.71505
2 × Sr-O2	2.90800
2 × Sr-O2	2.88649
2 × Sr-O2	2.69292
4 × O2-Te-O2	90
2 × O2-Te-O2	180
1 × O1-Te-O1	180
8 × O1-Te-O2	90

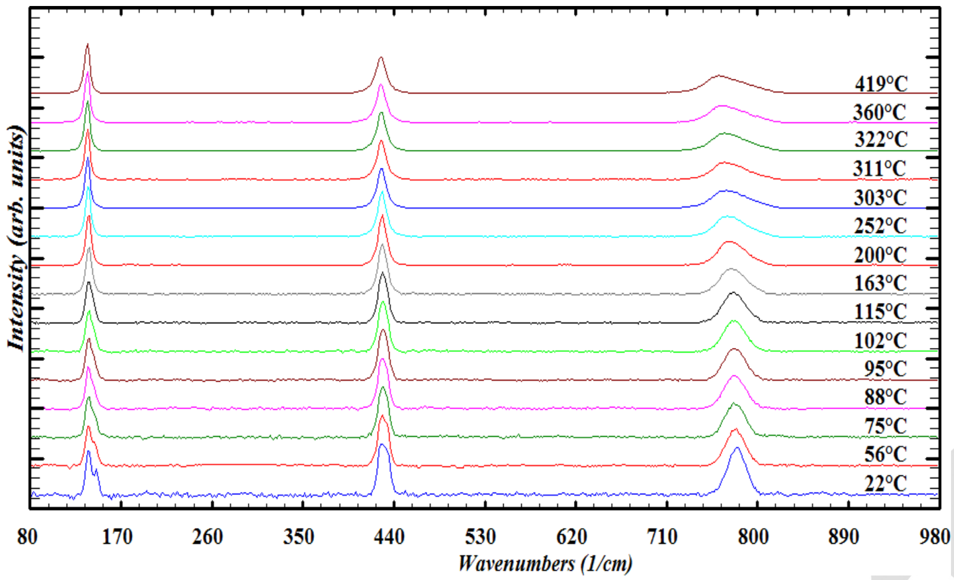

FIG. 4. Raman spectra of Sr_2MgTeO_6 obtained for selected temperatures, as indicated.

Mg^{2+} and Te^{6+} have octahedral coordination with the Mg–O bond lengths ranging between 2.032 and 2.065 Å and the Te–O bonds range within 1.904–1.941 Å.

Raman spectra of Sr_2MgTeO_6 were collected *in-situ* at room-pressure and elevated temperatures, up to 550 °C (Fig. 4). The observed Raman modes in the Sr_2MgTeO_6 specimen, recorded at ambient temperature, can be classified into three general families of lattice vibrations: Sr^{+2} translations, as well as translational and rotational modes of the TeO_6 octahedra, at wavenumbers below 200 cm^{-1}; O–Te–O bending vibrations, in the 200–500 cm^{-1} region; and Te–O stretching modes, at wavenumbers over 500 cm^{-1}.

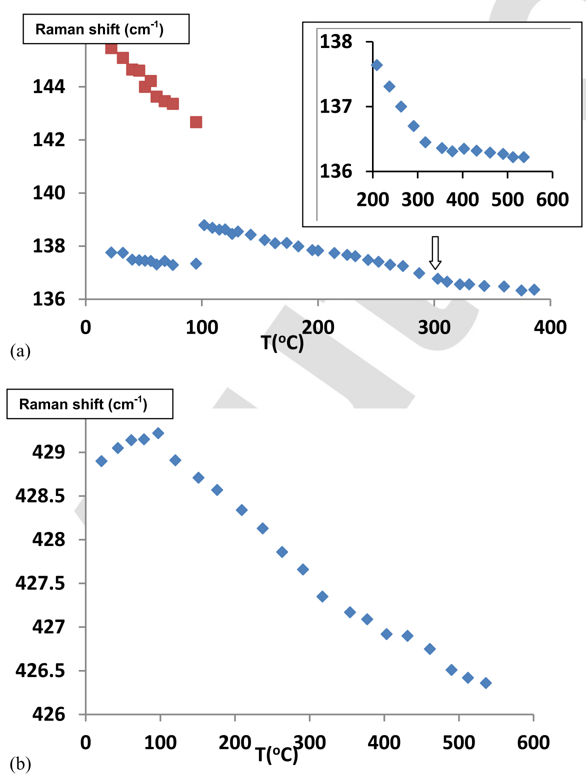

FIG. 5. Temperature dependencies of the Raman modes of Sr_2MgTeO_6. Discontinuity and slope change are observed around 100 °C and 300 °C. The inset shows results of repeated experiment.

Raman spectra have been deconvoluted with a computer program "LABSPEC," the main advantage of the program is that convergence is quite rapid compared with other refinement techniques. The temperature-dependence of the external and bending modes of Sr_2MgTeO_6 are presented in Fig. 5. The data collected in the temperature range of 25–400 °C are presented in (Fig. 5(a)), the modes centered at 138 cm^{-1}, 146 cm^{-1}, merge at around 100 °C indicating the first phase transition from the monoclinic (*I*2/*m*) to tetragonal (*I*4/*m*) structure. Upon further increasing temperature, around 300 °C, a major change in the slope of the temperature dependence of the mode centered at 138 cm^{-1} is observed (Fig. 5(a) and inset). In addition, a small but noticeable change in the slope of the temperature dependence of mode centered at 429 cm^{-1} is also detected at the same temperature (Fig. 5(b)). These observations indicate occurrence of a second phase transition from the tetragonal (*I*4/*m*) to cubic (*Fm*-3 *m*) structure. The temperature dependence of the intensity ratio, I_{780}/I_{138}, of two phonon modes 780 cm^{-1} and 138 cm^{-1}, was also examined. This ratio behaves linearly as a function of temperature, exhibiting a discontinuity in the slope at 100 °C (Fig. 6); thus showing occurrence of the first phase transition. The transition from tetragonal (*I*4/*m*) to cubic (*Fm*-3 *m*) phase is accompanied by a considerable change in the temperature dependence of this ratio around 300 °C (Fig. 6).

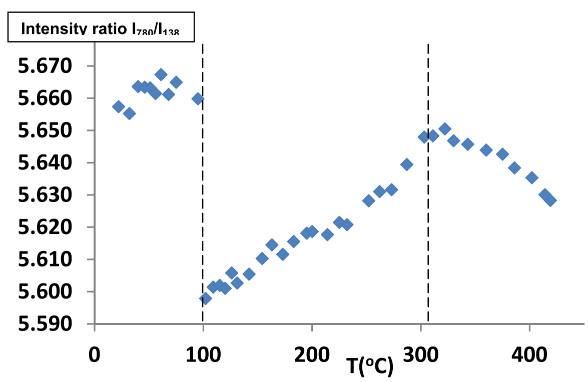

FIG. 6. I_{780}/I_{138} intensity ratio of two phonon modes in Raman spectra in Sr_2MgTeO_6. Two distinct changes occur at around 100 °C and 300 °C.

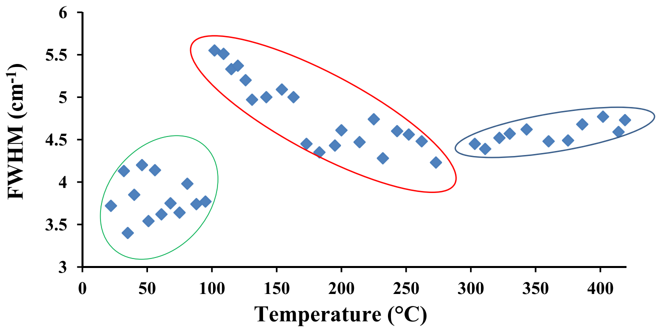

FIG. 7. FWHM for the 138 cm^{-1} external mode for Sr_2MgTeO_6 showing the first and second phase transitions (monoclinic to tetragonal to cubic). When the temperature reached around 100 °C, a break in the slope of the width of the mode was observed; thus, showing the first phase transition occurrence; a considerable change in the slope of the temperature dependence of the mode is observed around 300 °C, illustrating the second phase transition in Sr_2MgTeO_6.

The 138 cm^{-1} Raman mode becomes narrower at higher temperatures, indicating that it has become a single mode. To better understand the phase transitions in Sr_2MgTeO_6, the temperature-dependence of the FWHM quantified form of this mode is plotted in Fig. 7. The FWHM behaves in a linear way as a function of temperature; when the temperature reached around 100 °C, a break in the slope of the width of the modes was observed; thus, showing the first phase transition occurrence; a considerable change in the slope of the temperature dependence of the mode is observed around 300 °C, illustrating the second phase transition in Sr_2MgTeO_6.

Our systematic phase transition studies by XRD and Raman methods provide data about the stable structures at varied temperatures up to 550 °C. At room temperature, our XRD and Raman data confirmed that Sr_2MgTeO_6 is monoclinic with space group *I*2/*m*, which is consistent with those reported by Ubic *et al.*[15] On the other hand, Dias *et al.*[13] and Ubic *et al.*[14] reported that Sr_2MgTeO_6 is tetragonal, which matches our high temperature phase between 100 °C and 300 °C. Upon further heating to above 300 °C, we noticed the cubic phase with space group Fm-3 m, as reported previously by Bayer.[12] The obtained results agree well with those published by Ubic *et al.*,[15] who report the monoclinic crystal structure of Sr_2MgTeO_6, space group *I*2/*m*. On the other hand, findings of this study are inconsistent with reports by Dias *et al.*[13] and Ubic *et al.*,[14] claiming the tetragonal structure, and with Bayer[12] who solved the structure of in a cubic system. AQ4

The authors are grateful to The Swedish Foundation for International Cooperation in Research and Higher Education (STINT), The Swedish Research Council, and the Swedish International Development Co-operation Agency (Sida) for the financial grant (MENA) offered in support of this work. Finally, we would like to acknowledge University Hassan 1er and FSTS, Settat, Morocco, for their support. HPSynC is supported as part of EFree, an Energy Frontier Research Center funded by the U.S. Department of Energy (DOE), Office of Science under award number DE-SC0001057. AQ5

[1]R. E. Newnham and G. R. Ruschau, J. Am. Ceram. Soc. **74**, 463 (1991).
[2]R. J. Cava, R. B. van Dover, B. Batlogg, and E. A. Rietman, Phys. Rev. Lett. **58**, 408 (1987).
[3]J. J. Capponi, C. Chaillout, A. W. Hewat, P. Lejay, M. Marezio, N. Nguyen, B. Raveau, J. L. Soubeyroux, J. L. Tholence, and R. Tournier, Europhys. Lett. **3**, 1301 (1987).
[4]G. Q. Gong, C. Canedy, G. Xiao, J. Z. Sun, A. Gupta, and W. J. Gallagher, Appl. Phys. Lett. **67**, 1783 (1995).
[5]K. Ramesha, V. Thangadurai, D. Sutar, S. V. Subramanyam, G. N. Subbanna, and J. Gopalakrishnan, Mater. Res. Bull. **35**, 559 (2000).
[6]S. Nomura, K. Toyama, and K. Kaneta, Jpn. J. Appl. Phys., Part 1 **21**, L624 (1982). AQ6
[7]M. R. Varma, R. Resmi, and M. T. Sebastian, Jpn. J. Appl. Phys., Part 1 **44**, 298 (2005).
[8]G. Subodh and M. T. Sebastian, J. Am. Ceram. Soc. **90**, 2266 (2007).
[9]M. Udovic, M. Valant, and D. Suvorov, J. Euro. Ceram. Soc. **21**, 1735 (2001).
[10]D. K. Kwon, M. T. Lanagan, and T. R. Shrout, J. Am. Ceram. Soc. **88**, 3419 (2005).
[11]G. Subodh, R. Ratheesh, M. V. Jacob, and M. T. Sebastian, J. Mater. Res. **23**, 1551 (2008).
[12]G. Bayer, J. Am. Ceram. Soc. **46**, 604 (1963).
[13]A. Dias, G. Subodh, M. T. Sebastian, M. M. Lage, and R. L. Moreira, Chem. Mater. **20**, 4347 (2008).
[14]R. Ubic, S. Letourneau, S. Thomas, G. Subodh, and M. T. Sebastian, Chem. Mater. **22**, 4572 (2010).
[15]R. Ubic, S. Letourneau, S. Thomas, G. Subodh, and M. T. Sebastian, J. Aus. Ceram. Soc **47**, 49 (2011). AQ7
[16]J. Rodriguez-Carvajal, *Collected Abstracts of Powder Diffraction Meeting* (Toulouse, France, 1990), Vol. 127.
[17]T. Roisnel and J. R.-Carvajal, Mater. Sci. Forum **378**, 118 (2001).
[18]M. Azdouz, B. Manoun, M. Azrour, L. Bih, L. El Ammari, S. Benmokhtar, and P. Lazor, J. Mol. Struct. **963**, 258 (2010).
[19]H. Bih, L. Bih, B. Manoun, M. Azdouz, S. Benmokhtar, and P. Lazor, J. Mol. Struct. **936**, 147 (2009).
[20]A. Boultif and D. Louër, J. Appl. Crystallogr. **24**, 987 (1991).
[21]W. T. Fu, S. Akerboom, and D. J. W. IJdo, J. Alloys Compd. **476**, L11 (2009).